J Fluoresc (2015) 25:835–848
DOI 10.1007/s10895-015-1549-6

ORIGINAL PAPER

Novel 6-(1H-benzo[d]imidazol-2-yl) benzo[a]phenazin-5-ol Derivatives with Dual Emission and Large Stokes Shift Synthesis, Photophysical Properties and Computational Studies

Amol S. Choudhary · Nagaiyan Sekar

Received: 15 December 2014 / Accepted: 23 February 2015 / Published online: 12 April 2015

Abstract Novel phenazine containing dyes were obtained by the condensation of *5-hydroxybenzo[a]phenazine-6-carbaldehyde* and *5-chloro-benzo[a]phenazine-6-carbaldehyde* with 1,2-diaminobenzene. The dyes were characterized by FT-IR, 1H NMR, elemental analysis and mass spectra. The UV–vis absorption and fluorescence emission spectra of the dyes were studied in solvents of differing polarity; the dyes exhibited excited state intra molecular proton transfer. The structural changes due to excited state intramolecular proton transfer (ESIPT) phenomenon in terms of bond angle, bond distances and geometry were investigated with the help of DFT computations. The computed absorption and emission were in agreement with the experimental absorption and emission.

Keywords ESIPT · DFT · Benzimidazole · Phenazine · Photophysical properties

Introduction

The excited state intramolecular proton transfer (ESIPT) is a class of proton transfer reactions occuring at the excited state that can be initiated by the absorption of light. It represents one of the most basic processes implicated in chemical as well as in living systems [1, 2]. The molecules exhibiting ESIPT have been exploited as model systems for the study of the proton transfer reaction dynamics [3, 4]. The ESIPT reaction, a fast enol-to-keto or (amine-to-imine) prototropy occurring in the excited states of intramolecularly hydrogen-bonded molecules, has been extensively investigated because of its fundamental interest in photophysical properties and potential applications in luminescent materials [5], photo patterning [6], chemosensors [7], proton transfer laser [8], photo stabilizers [9, 10], molecular logic gates [11], molecular probes [12], metal ion sensors [13, 14], radiation hard-scintillator counters [15], and organic light emitting devices (OLEDs) [16, 17], The ESIPT compounds have also drawn much attention due to their potential applications in optical devices [18, 19] that may take advantage of the salient properties of the ESIPT compounds such as the ultra-fast reaction rate and extremely large fluorescence Stokes shift [20] compared to the normal fluorophores such as fluorescein, rhodamine or boron dipyrromethene (BODIPY), coumarin [21–23].

The structural and electronic configuration of the excited tautomer (ESIPT product) differs from the original one, and is characterized by an abnormally large Stokes shift of fluorescence. In this research, we synthesized novel ESIPT chromophores - 6-(1H-benzo[d]imidazol-2-yl)benzo[a]phenazin-5-ol, hydroxy substituted benzophenazine fused imidazole (HPI) and its chloro-containing derivative (HPI-Cl) (Fig. 1 and Scheme 1). The molecular geometry and spectroscopic properties of the synthesized molecules have been investigated using the optimized geometries of the molecules obtained using DFT computations

They exhibit intense blue-red fluorescence at 460–540 nm. We found that the structural and electronic features provided by DFT/ B3LYP 6–311 G (d) calculations describe well the mechanism for ESIPT, yielding conformer assignment consistent with the experimental observations.

Electronic supplementary material The online version of this article (doi:10.1007/s10895-015-1549-6) contains supplementary material, which is available to authorized users.

A. S. Choudhary · N. Sekar (✉)
Institute of Chemical Technology, Matunga, Mumbai 400019, India
e-mail: n.sekar@ictmumbai.edu.in

N. Sekar
e-mail: nethisekar@gmail.com

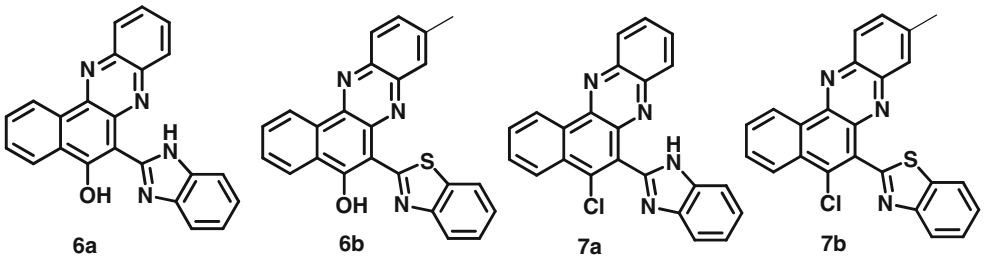

Fig. 1 Structures of the dyes 6a, 6b, 7a and 7b

Experimental Section

Materials and Equipment

2-Hydroxy-1, 4-napthaquinone, substituted o-phenylenediamine, were procured from Sigma Aldrich. The reactions were monitored by TLC using 0.25 mm E-Merck silica gel 60 F254 percolated plates, which were visualized with UV light. Melting points were measured on standard melting point apparatus from Sunder industrial product Mumbai, and are uncorrected. The FTIR spectra were recorded on a Perkin-Elmer Spectrum 100 FTIR Spectrometer. 1H NMR spectra were recorded on VXR

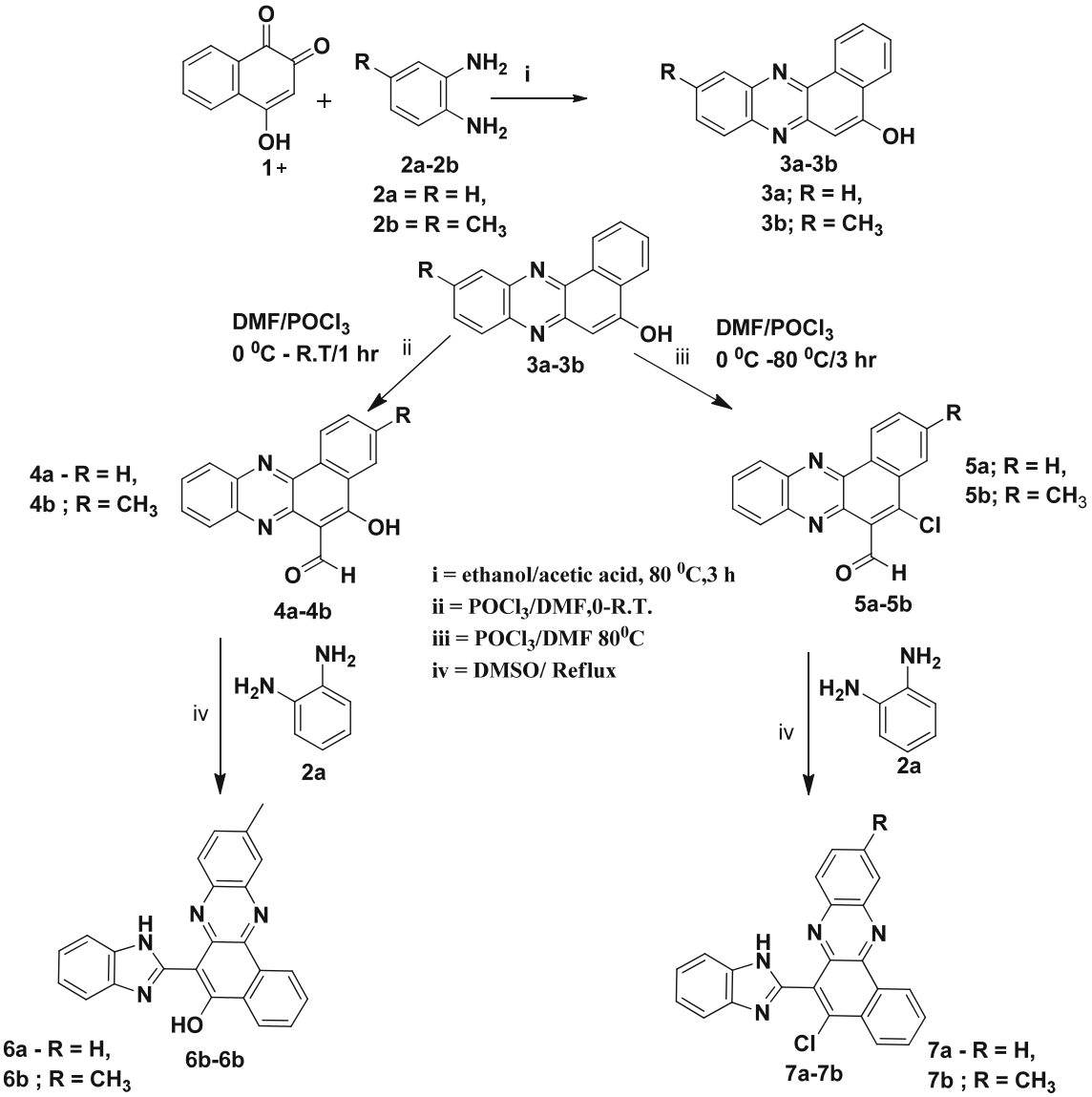

Scheme 1 Synthesis of 6-(1H-benzo[d] imidazol-2-yl) benzo[a] phenazin-5-ol Derivatives 6a, 6b, 7a and 7b

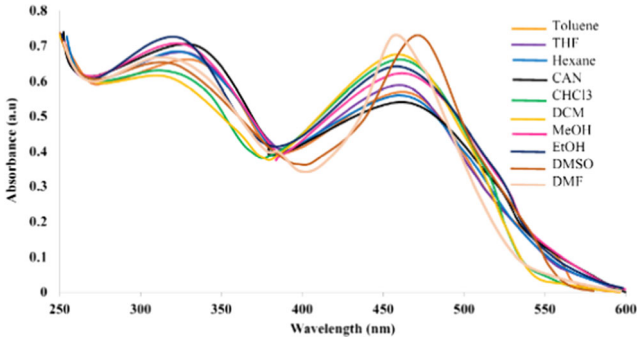

Fig. 2 Absorption spectra of 6a in different protic and aprotic solvents

300 MHz instrument using TMS as an internal standard. The visible absorption spectra of the compounds were recorded on a Spectronic Genesys 2 UV-Visible spectrophotometer. The emission and excitation spectra of the compounds were measured on Varian Cary eclipse spectrofluorimeter.

Quantum Yield Calculation

Quantum yield of compounds 6a, 6b, 7a and 7b were determined by using fluroscien as standard. Absorption and emission characteristics of standard as well as unknown samples were measured at different concentration of unknown samples and standard at (2, 4, 6, 8 and 10 ppm level). Absorbance intensity values were plotted against emission intensity values. A linear plot was obtained. Gradients were calculated for each unknown compound and for standard. All the measurements were done by keeping the parameters such as solvent and slit width constant. Relative quantum yield of all synthesized compounds 6a, 6b, 7a and 7b were calculated by using the Formula 1 [23, 24]

Formula 1: Relative fluorescence quantum yield

$$\Phi_x = \Phi_{std}(\mathrm{Grad\,x}/\mathrm{Grad\,st})\left(\eta^2{}_x/\eta^2{}_{st}\right)$$

Where;

Φ_X Quantum yield of unknown sample

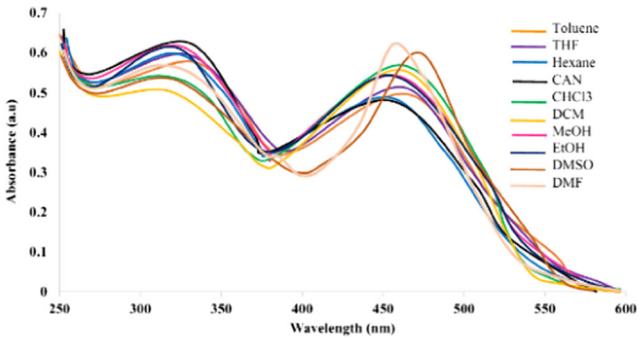

Fig. 3 Absorption spectra of 6b in different protic and aprotic solvents

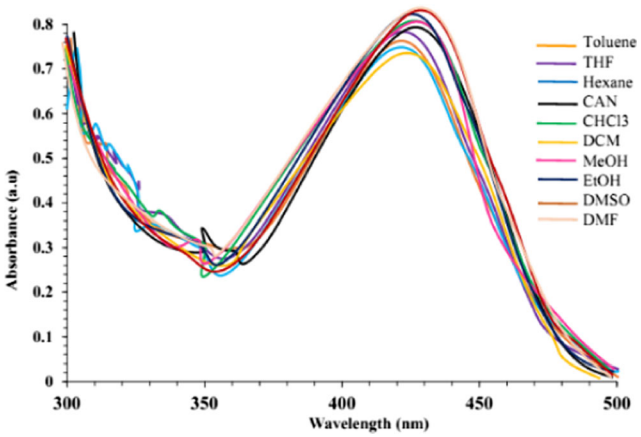

Fig. 4 Absorption spectra of 7a in different protic and aprotic solvents

Φ_{ST} Quantum yield of standard used
Grad_X Gradient of unknown sample
Grad_X Gradient of standard used
$\eta^2{}_{st}$ Refractive index of solvent for standard sample
$\eta^2{}_x$ Refractive index of solvent for sample

Computational Methods

Gaussian 09 program package was used to optimize geometry and to study the synthesized azo dyes in their enol and keto tautomeric forms [25]. Ground state (S0) geometry of the dyes as an isolated molecule and in solvent environments were optimized in their C1 symmetry using DFT [26]. The Becke's three parameter exchange functional (B3) [27] combining with nonlocal correlation functional by Lee, Yang and Parr (LYP) [28] and the basis set 6-31G (d) was used for all the atoms. Same method was used for vibrational analysis to verify that the optimized structures correspond to local minima on the energy surface. Time Dependent Density Functional Theory (TD- DFT) computations were used to obtain the vertical excitation energies and oscillator strengths at the

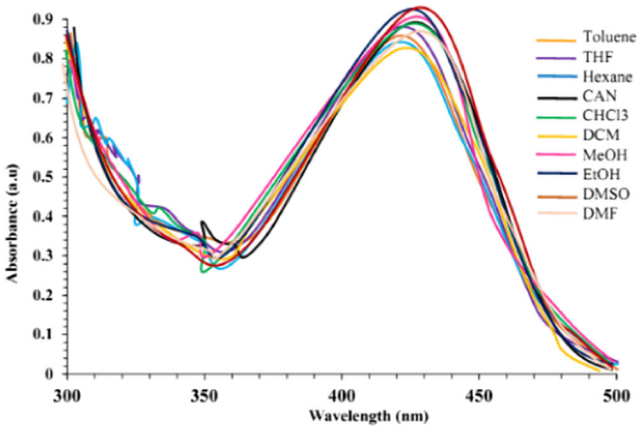

Fig. 5 Absorption spectra of 7b in different protic and aprotic solvents

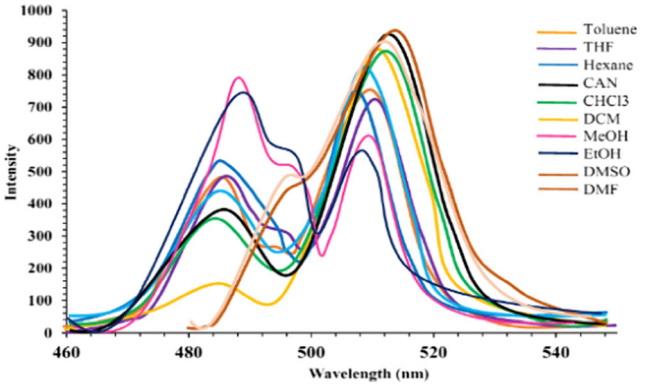

Fig. 6 Emission spectra of 6a in different protic and aprotic solvents

optimized ground state equilibrium geometries at the same level of theory [29–31]. All the computations in solvents of different polarities were carried out using the Self-Consistent Reaction Field (SCRF) method and the Polarizable Continuum Model (PCM) [32].

Synthesis and Characterization

General Method for the Synthesis and Characterization of 3a and 3b

2-Hydroxy-1, 4-napthaquinone 1 (2 mol) and substituted o-phenylenediamine 2a-2b (2 mol) were stirred in a mixture of AcOH: EtOH (50:50) (20 ml) at 80 °C for 1–1.5 h. The progress of the reaction was monitored by TLC. After completion of the reaction, the reaction mass was poured in to the crushed ice and stirred for 30 min at room temperature. The reaction mass was filtered and the product was purified by column chromatography using silica gel 100–200 mesh and ethyl acetate: hexane (50:50) as eluent system.

General Method for the Synthesis and Characterization of 4a and 4b

$POCl_3$ (0.015 mol) was added to DMF (0.20 mol) at 0 °C within 15 min and stirred for 30 min at 0 °C. Naphtho [1,2-a]phenazin-5-ol 3a or 3b (0.01 mol) dissolved in DMF (5 ml) was added slowly at 0–5 °C and stirred for 30 min. The reaction mixture was then stirred at room temperature for 3 h and completion of the reaction was monitored by TLC. The reaction mass was poured in ice and stirred, neutralized with sodium bicarbonate, filtered and dried. The crude aldehyde was recrystallized from ethanol and purified by column chromatography using silica gel 100–200 mesh and ethyl acetate: hexane (10:90) as eluent system.

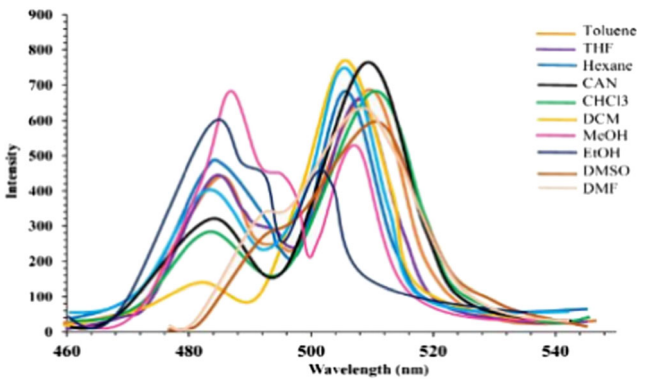

Fig. 7 Emission spectra of 6b in different protic and aprotic solvents

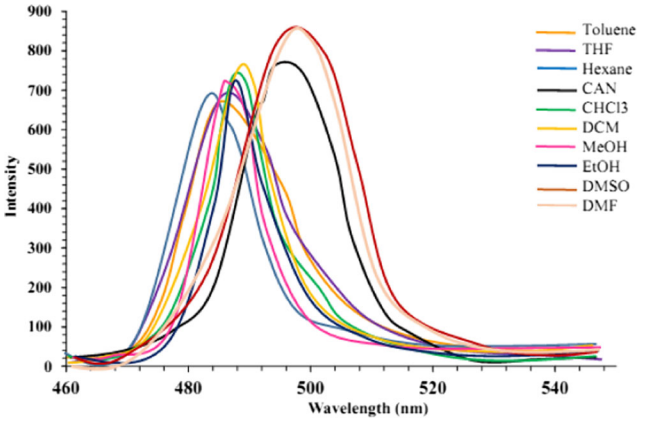

Fig. 8 Emission spectra of 7a in different protic and aprotic solvents

Synthesis of 5-Hydroxybenzo[a]phenazine-6-carbaldehyde4a Yield=69 %, Melting point: 166–168 °C FT-IR (KBr, cm^{-1}): 3100 (−OH), 2930 (COH), 1600 (CO), 1577 (C=N), 1200 (C-O). 1H NMR ($CDCl_3$, 500 MHz)=δ 7.782 (dd, 4H, J=6.9, 4.7 Hz, Ar-H), 7.212 (dd, 4H, J=7.4, 5.1 Hz, Ar-H), 8.60 (bs, 1H,-OH), δ 8.2 (s, 1H, Aldehyde -CHO) ppm. Mass: m/z 274.13 [M+1].

Synthesis of 5-Hydroxy-10-methylbenzo[a]phenazine-6-carbaldehyde 4b Yield=65 %, Melting point: 173–177 °C, FT-IR (KBr, cm^{-1}): 3100 (−OH), 2930 (COH), 1600 (C=O), 1577 (C=N), 1200 (C-O). 1H NMR ($CDCl_3$, 500 MHz)=δ 2.67 (s, 3H, $-CH_3$), 7.83 (m, 4H, J=7.4, 5.1 Hz, Ar-H), 7.29 (m, 4H, Ar-H), 8.60 (bs, 1H, −OH), 8.5 (s, 1H) ppm. Mass: m/z 288.24 [M+1].

General Method for the Synthesis of 5a and 5b

$POCl_3$ (0.035 mol) was added to DMF (0.20 mol) at 0 °C within 15 min and stirred for 30 min at 0 °C. Naphtho [1,2-a]phenazin-5-ol 3a-3b (0.01 mol) dissolved in DMF (5 ml) was added slowly at 0–5 °C and stirred for 30 min. The reaction mixture was then heated to 80–90 °C for 3–3.5 h and completion of the reaction was monitored by TLC. The reaction mass was poured in ice and stirred neutralized with sodium bicarbonate, filtered and dried. The crude aldehyde was recrystallized from ethanol and the product was purified by

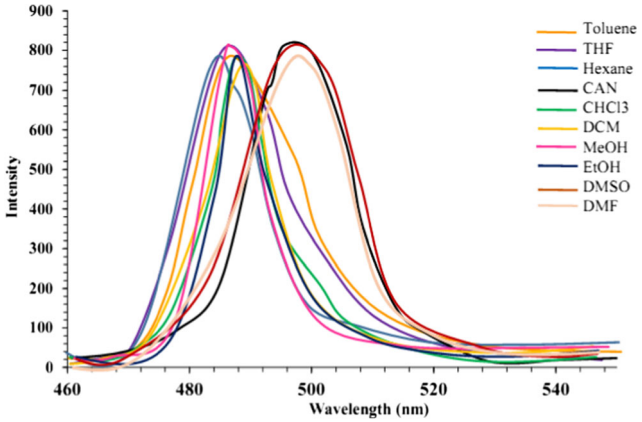

Fig. 9 Emission spectra of 7b in different protic and aprotic solvents

column chromatography using silica gel 100–200 mesh and hexane as eluent system.

General Method for the Synthesis of 5a and 5b $POCl_3$ (0.035 mol) was added to DMF (0.20 mol) at 0 °C within 15 min and stirred for 30 min at 0 °C. Naphtho [1,2-a]phenazin-5-ol 3a-3b (0.01 mol) dissolved in DMF (5 ml) was added slowly at 0–5 °C and stirred for 30 min. The reaction mixture was then heated to 80–90 °C for 3–3.5 h and completion of the reaction was monitored by TLC. The reaction mass was poured in ice and stirred neutralized with sodium bicarbonate, filtered and dried. The crude aldehyde was recrystallized from ethanol and product was purified by column chromatography using silica gel 100–200 mesh and hexane as eluent system.

Synthesis of 5-Chlorobenzo[a]phenazine-6-carbaldehyde 5a Yield=55 %, Melting point: 157–159 0C, FT-IR (KBr, cm^{-1}): 3012 (Ar-H), 2937 (C-H), 2927 (COH), 1611 (CO), 1580 (C=N), 1208 (C-O), 786 (C-Cl) cm-1. 1H NMR ($CDCl_3$, 500 MHz)=δ 7.782 (dd, 4H, J=6.9, 4.7 Hz, Ar-H), 7.212 (dd, 4H, J=7.4, 5.1 Hz, Ar-H), δ 8.2 (s, 1H, Aldehyde -CHO) ppm. Mass: m/z 306.64 [M+1].

Synthesis of 5-Chloro-10-methylbenzo[a]phenazine-6-carbaldehyde 5b Yield=59 %, Melting point: 154–156 0C FT-IR (KBr, cm^{-1}): 2930 (COH), 1610 (CO), 1581 (C=N), 1208 (C-O), 786 (C-Cl) cm^{-1}. ^1H NMR ($CDCl_3$¬¬, 500 MHz)=δ 7.782 (dd, 4H, J=6.9, 4.7 Hz, Ar-H), 7.212 (dd, 4H, J=7.4, 5.1 Hz, Ar-H), δ 8.2 (s, 1H, Aldehyde -CHO) ppm. Mass: m/z 292.21 [M+1].

Table 1 Absorption, emission and quantum yield of synthesized compounds 6a, 6b, 7a and 7b in Toulene solvent

Compounds	λ_{abs}	λ_{em} short	Stoke shift cm^{-1}	Φ_F	λem long	Stoke shift cm^{-1}	Φ_F
6a	460	485	400,000	0.001	520	125,000	0.22
6b	463	480	434782.61	0.001	525	121951.22	0.187
7a	440	485	222222.22	0.41	–	——	—
7b	440	485	222222.22	0.389	—	——	–

General Method for the Synthesis of 6a-6b and 7a-7b

6-(1H-benzo[d]imidazol-2-yl)-10-methylbenzo[a]phenazin-5-ol 6a 5-Hydroxy-10-methylbenzo[a]phenazine-6-carbaldehyde (0.01 mol, 0.29 gm) and o-phenylenediamine 2a (0.01 mol, 0.11 gm) were stirred in DMSO at 90 °C for 2–2.5 h. The progress of the reaction was monitored by TLC. After completion of the reaction, the reaction mass was poured in to the crushed ice and stirred for 30 min at room temperature. The reaction mass was filtered and the product was purified by column chromatography using silica gel 100–200 mesh and ethyl acetate: hexane (20:80) as eluent system.

Yield=54 %, Melting point: 157–159 °C FT-IR (KBr, cm-1): 3330 (−NH), 1610 (CO), 1581 (C=N), 1208 (C-O), 786 (C-Cl) cm-1. 1H NMR ($CDCl_3$, 500 MHz)=δ 7.782 (dd, 4H, J=6.9, 4.7 Hz, Ar-H), 7.212 (dd, 4H, J=7.4, 5.1 Hz, Ar-H), δ 8.2 (dd, 2H, Ar-H), δ 8.56 (dd, 2H, Ar-H), δ 9.3 (s,1H, −OH),, δ 6.3 (s,1H, −NH) ppm. Mass: m/z 362.21 [M+1].

6-(1H-benzo[d]imidazol-2-yl)benzo[a]phenazin-5-ol 6b 5-Hydroxy-10-methylbenzo[a]phenazine-6-carbaldehyde (0.01 mol, 0.29 gm) and o-phenylenediamine 2a (0.01 mol, 0.11 gm) were stirred in DMSO at 90 °C for 2–2.5 h. The progress of the reaction was monitored by TLC. After completion of the reaction, the reaction mass was poured in to the crushed ice and stirred for 30 min at room temperature. The reaction mass was filtered and the product was purified by column chromatography using silica gel 100–200 mesh and ethyl acetate: hexane (20:80) as eluent system.

Yield=59 %, Melting point: 164–166 °C FT-IR (KBr, cm^{-1}): 3330 (−NH), 1610 (CO), 1581 (C=N), 1208 (C-O), 786 (C-Cl) cm-1. 1H NMR ($CDCl_3$, 500 MHz)=δ 2.67 (s, 3H, $-CH_3$),δ 7.782 (dd, 4H, J=6.9, 4.7 Hz, Ar-H), 7.212 (dd, 4H, J=7.4, 5.1 Hz, Ar-H), δ 8.2 (dd, 2H, Ar-H), δ 8.56 (dd, 2H, Ar-H), δ 9.3 (s,1H, −OH),, δ 6.3 (s,1H, −NH) ppm. Mass: m/z 376.21 [M+1].

6-(1H-benzo[d]imidazol-2-yl)-5-chloro-10-methylbenzo[a]phenazine 7a 5-Chloro-10-methylbenzo [a]phenazine-6-carbaldehyde (0.01 mol, 0.31 gm) and o-phenylenediamine 2a (0.01 mol, 0.11 gm) were stirred in a DMSO solvent at 90 °C for 2–2.5 h. The progress of the reaction was monitored by TLC. After completion of the reaction, the reaction mass was poured in to the crushed ice and stirred for 30 min at room temperature. The reaction mass was filtered and the product was purified by column

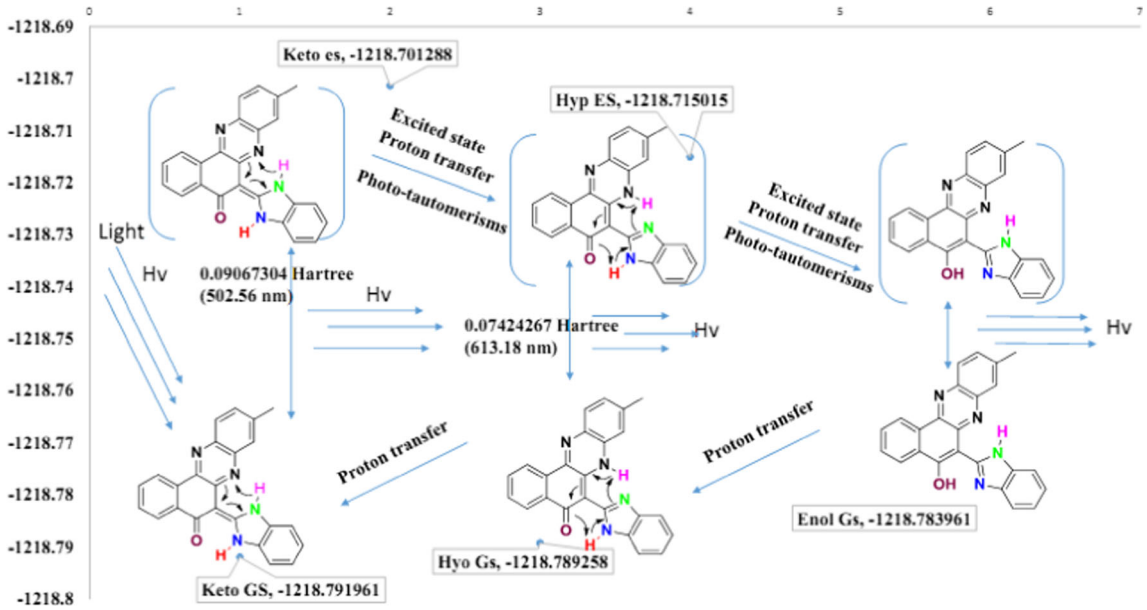

Fig. 10 ESIPT in 6b occurring along the pre-existing hydrogen bond in the ground state between the phenolic -OH group and the quinonoid oxygen of the dye

chromatography using silica gel 100–200 mesh and ethyl acetate: hexane (20:80) as eluent system.

Yield=53 %, Melting point: 181–186 °C FT-IR (KBr, cm^{-1}): 3220 (NH), 1610 (C=O), 1592 (C=N), 1231 (C-O), 778 (C-Cl) cm^{-1}. ^{1}H NMR ($CDCl_3$, 500 MHz)=δ 8.4 (dd,2H, Ar-H), δ 7.981(dd,2H,Ar-H), δ 7.782 (dd, 4H, J=6.9, 4.7 Hz, Ar-H), 7.212 (dd, 4H, J=7.4, 5.1 Hz,ArH),δ 10.1 (s, 1H, −NH) ppm. Mass: m/z 380.90 [M+1].

6-(1H-benzo[d]imidazol-2-yl)-5-chlorobenzo[a]phenazine 7b 5-Chlorobenzo[a]phenazine-6-carbaldehyde 4a (0.01 mol, 0.38 gm) and o-phenylenediamine 2a (0.01 mol, 0.11 gm) were stirred in a DMSO solvent at 90 °C for 2–2.5 h. Completion of the reaction was monitored by TLC. After completion of the reaction, the reaction mass was poured in to the crushed ice and stirred for 30 min at room temperature. The reaction mass was filtered and the product was purified by column chromatography using silica gel 100–200 mesh and ethyl acetate: hexane (20:80) as eluent system.

Yield=49 %, Melting point: 195–196 °C FT-IR (KBr, cm^{-1}): 3227 (NH), 1605 (C=O), 1580 (C=N), 1226 (C-O), 778 (C-Cl) cm^{-1}. ^{1}H NMR ($CDCl_3$, 500 MHz)=δ 2.537 (s, 3H, $-CH_3$),δ 8.4 (dd,2H,Ar-H), δ 7.981(dd,2H,Ar-H), δ 7.782 (dd, 4H, J=6.9, 4.7 Hz, Ar-H), 7.212 (dd, 4H, J=7.4, 5.1 Hz, ArH),δ 10.1 (s, 1H, −NH) ppm. Mass: m/z 395.40 [M+1].

Results and Discussion

Synthesis Strategy and Characterization

The synthetic plan for the preparation of 6-(1H-benzo[d]imidazol-2-yl)-benzo[a]phenazin-5-ol 6a-6b and 7a-7b is shown in Scheme 1. Benzo[a]phenazin-5-ol 3a and 3b were prepared by the condensation of 2-hydroxy-1, 4-napthaquinone (Lawson) 1 with the substituted 1, 2-diaminobenzene 2a and 4-methylbenzene-1, 2-diamine 2b in the presences of glacial acetic acid at 60 °C for 60 min. 5-Hydroxybenzo[a]phenazine-6-

Table 2 Computed bond length, dihedral angle and bond angle of enol and keto form of 6a

L	enol	Keto	D^0	Enol	Keto	θ^0	enol	Keto
H14-N2	2.030 (1.826)	1.960 (1.872)	N4-H14-N2-C3	0.019	0.007 (0.004)	C1-O1-H9	108.969	108.312 (110.614)
N4-H14	1.014 (1.035)	1.019 (1.029)	N4-C17-C2-C3	0.00	−0.022 (−0.001)	O1-H9-N3	147.678	126.270 (124.65)
N3-H9	1.646 (1.705)	1.019 (1.0188)	N4-C17-C2-C1	179.988	179.982 (179.999)	N4-C17-C2	125.367	127.056 (126.262)
H9-O1	1.008 (0.995)	1.874 (1.891)	N3-C17-C2-C1	0.021	−0.008 (−0.0011)	N3-C17-C2	123.201	26.460 (126.4687)
C17-C2	1.457 (1.417)	1.425 (1.418)	N3-C17-C2-C3	−179.987	−0.020 (179.999)	H14-N4-C17	121.439	118.945 (117.428)

L bond length (interatomic distance between atom in Å), D^0 Dihedral angle, θ^0 Bond angle

Atom no. is depicted in Fig. 11

Table 3 Optimized geometry parameters of Enol 6b,Keto 6b and hydrophenazine (Hyp) 6b in DMF solvent in the ground state. (bond lengths are in Å, angles are in °)

L		enol	Keto	Hyp	D^0	Enol	Keto	Hyp	θ^0	enol	Keto	Hyp
H13-N2	S0	2.032	1.967	1.035	N4-H13-N2-C3	−0.022	96.867	0.003	C1-O1-H8	108.86	108.24	108.601
	S1		1.869	1.027			0.009	0.006			110.62	109.486
N4-H13	S0	1.015	1.019	1.796	N4-C17-C2-C3	−0.014	0.007	0.002	O1-H8-N3	147.84	126.00	2.649
	S1		1.030	1.847			0.002	0.001			124.75	125.991
N3-H8	S0	1.645	1.018	1.014	N4-C17-C2-C1	179.98	−179.998	179.998	N4-C17-C2	125.44	127.14	125.331
	S1		1.019	1.018			−179.998	179.998			126.28	126.131
H8-O1	S0	1.008	1.881	1.945	N3-C17-C2-C1	0.004	0.001	0.00	N3-C17-C2	27.064	126.47	27.450
	S1		1.888	1.861			−0.001	0.002			126.43	123.372
C17-C2	S0	1.458	1.427	1.455	N3-C17-C2-C3	0.003	−0.004	0.002	H13-N4-C17	121.56	119.28	99.677
	S1		1.419	1.420			−0.004	179.998			117.36	98.703
N3-O1	S0	2.555	2.613	2.649					N4-H13-N2			26.940
	S1		2.607	2.594								15.078
N4-N2	S0	2.722	2.686	2.657								
	S1		2.635	2.690								

L bond length (interatomic distance between atom in Å), D^0 Dihedral angle, θ^0 Bond angle, *S0* Ground state energy, *S1* Excited state
Atom no. is depicted in Fig. 11

carbaldehyde 4a-4b and 5a-5b were prepared by the Vilsmeyer Haack reaction. The structures of the compounds were confirmed by FTIR, ^{1}HNMR, mass spectral analysis. The compounds 4a-4b and 5a-5b on treatment with 1,2-diamnobenzene 2a, respectively, in the presence of DMSO at reflux temperature (100–130 °C) for 4–5 h gave 6-(1H-benzo[d]imidazol-2-yl)benzo[a]phenazin-5-ol 6a, 6-(1H-benzo[d]imidazol-2-yl) -9-methylbenzo[a]phenazin-5-ol 6b, 6-(1H-benzo[d]imidazol-2-yl)-5-chlorobenzo[a] phenazine 7a and 6-(1H-benzo[d]imidazole-2-yl)-5-chloro- 9-methylbenzo[a]phenazine 7b. The synthesized compounds 6a-6b and 7a-7b were purified by column chromatography and the structures were confirmed by FTIR, ^{1}HNMR, and mass spectra. The compound 6a showed a distinct stretching vibrational peak for -OH in FTIR at 3252–3267 cm^{-1} and ^{1}HNMR showed the phenolic -OH signal at δ10.56 ppm and confirmed by D_2O exchange. The synthesized benzimidazole molecules which contain acidic hydroxy group at 5-position and phenazine fused at the 7th and 8th positions with respect to the basic -N=moiety. The location of these groups is in such a way that there is an intramolecular hydrogen bonding in the ground state. On excitation, the –N=moiety become strongly basic and –OH group as well as benzophenazine core becomes strongly acidic. This leads to the excited state intra-molecular proton transfer (ESIPT) and thus the formation of keto isomer (k1). The ESIPT reaction have been subject of numerous investigations in the literature but reported ESIPT reaction has very small fluorescence quantum yield and Stokes shift. It could be due to the lower acidic group (like -NH_2) attached to the donor aromatic ring system. This limitation has overcome by introducing -OH group as well as fused phenazine core group in system

Table 4 Ground state energy of enol and keto form 6a

	Energy of enol 6a=E_{enol}		Energy of keto 6a=E_{keto}		$\Delta E=E_{enol}-E_{keto}$	
Solvents	Hartree	eV	Hartree	eV	Hartree	eV
Gas	−1179.4479	−32093.040	−1179.4531	−32093.271	0.00524	0.2301939
THF	−1179.4556	−32093.035	−1179.4634	−32093.264	0.00784	0.2286701
Toluene	−1179.4520	−32093.031	−1179.4587	−32093.258	0.00667	0.2271300
Chloroform	−1179.4545	−32092.987	−1179.462	−32093.201	0.00747	0.2132421
Methanol	−1179.4574	−32092.956	−1179.4658	−32093.159	0.00840	0.2033267
Ethanol	−1179.4572	−32092.890	−1179.4656	−32093.072	0.00835	0.1815234
DMSO	−1179.458	−32092.77	−1179.4660	−32092.920	0.00846	0.1426675

E_{enol} Ground state Energy of enol, E_{keto} Ground state energy of keto, ΔE E_{enol} - E_{keto}

Table 5 Ground state energy of enol, hyp and keto form 6b

Solvents	E_{enol} Hartree	$E_{enol\ in}$ eV	E_{keto} in Hartree	E_{keto} in eV	E_{Hyp} in Hartree	E_{Hyp} in eV	E_{enol}-E_{keto}	E_{Hyp}-E_{keto}	E_{enol}-E_{Hyp}
Gas	−1218.7743	−33162.8478	−1218.7791	−33162.9794	−1218.7772	−33162.9272	0.1316	0.0522	0.0794
THF	−1218.7821	−33163.0618	−1218.7896	−33163.2643	−1218.7871	−33163.1968	0.2025	0.0675	0.1351
Toluene	−1218.7785	−33162.9630	−1218.7848	−33163.1339	−1218.7826	−33163.0756	0.1709	0.0582	0.1126
Chloroform	−1218.7810	−33163.0304	−1218.7881	−33163.2231	−1218.7857	−33163.1590	0.1927	0.0641	0.1286
Methanol	−1218.7840	−33163.1116	−1218.7920	−33163.3293	−1218.7893	−33163.2557	0.2177	0.0736	0.1441
Ethanol	−1218.7838	−33163.1066	−1218.7917	−33163.3227	−1218.7890	−33163.2498	0.2162	0.0729	0.1433
DMSO	−1218.7841	−33163.1166	−1218.7922	−33163.3357	−1218.7895	−33163.2615	0.2192	0.0742	0.1449

E_{enol} Energy of enol 6b, E_{keto} energy of Keto 6b, E_{hyp} Energy of Hydrophenazine (Hyp)

which increases the rate of intra-molecular proton transfer in the S1 state; synthesized compounds 6a-6b shows single absorption and dual emission with good fluorescence intensity and reasonably large Stokes shift; ESIPT reaction pathway is shown in Fig. 2. The phenolic -OH peak disappeared in D_2O exchange with an additional peak appearing at d 4.80–4.82 ppm. Mass spectral data for compound 6a show M+1 peak at 362.1, which is in good agreement with its molecular weight of M+1 species. Absorption and emission spectra were measured to investigate its photo-physical properties and also the solvatochromisms and solvatofluorism behavior of the molecule were studied by measuring electronic absorption and emission spectra in solvents of different polarities.

Optical Properties

The absorption spectra of 6a, 6b, 7a and 7b in different protic and aprotic solvents are shown in Figs. 2, 3, 4 and 5. In all the solvents, the lowest energy absorption band for the dye 6a and 6b appears as two absorption envelopes at ~340 and ~480 nm. This band assigned to the S0 to S1 transition of π -π^* nature having some charge transfer character as indicated from Figs. 2 to 3 the widths of the absorption spectra are fairly indistinguishable in all the solvents studied, and suggest that in all the solvent systems the dye in the ground state exclusively exists in a single conformational structure. While 7a and 7b show single absorption band at 430 nm as show in Figs. 4 and 5.

The fluorescence spectra of the dyes 6a, 6b, 7a and 7b in protic and aprotic solvents are shown in Figs. 6, 7, 8 and 9. As seen in all the solvents studied, the fluorescence spectra do not show any mirror image relationship with the absorption spectra, suggesting that the dye undergoes a large structural change in the excited state compared to its conformational structure in the ground state. It is evident from Figs. 6 to 7 that the emission spectra of the dyes 6a and 6b in the studied solvents are essentially composed of two emission bands, one with peak around 495 and 510 nm, and the other with peak around 500–510 nm (designated as the short wavelength emission band and the long wavelength emission band respectively, for the convenience of our discussions).

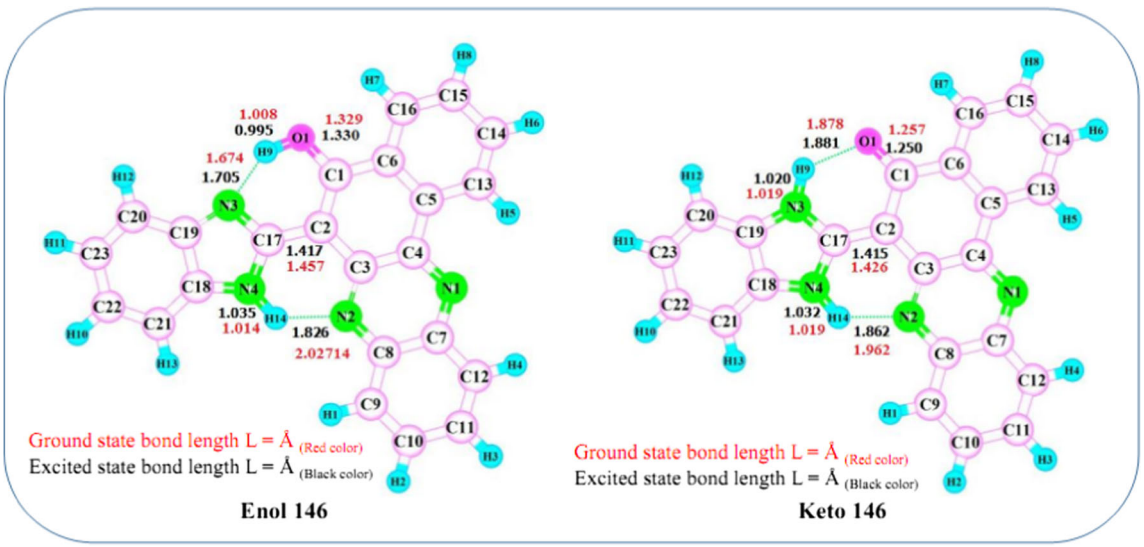

Fig. 11 Optimized geometry of enol and keto form of compound 6a

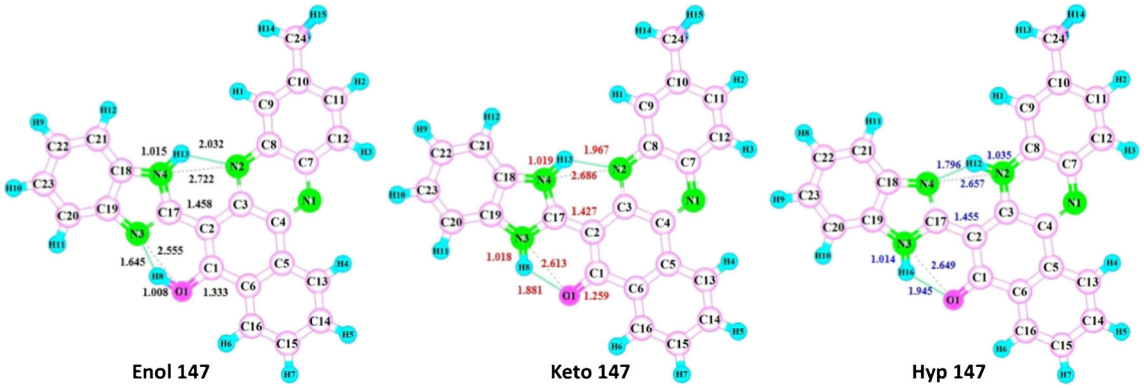

Fig. 12 Optimized geometry of enol,Keto and hydrophenazine (Hyp) form of compound 6b

The Stokes shifts of 6a and 6b are larger than 7a and 7b of the imidazole fluorophores. Since the spectra were measured under the same conditions thus we can anticipate high fluorescence quantum yields for 6a and 6b compared to 7a and 7b. Interestingly, dual emission bands at 485 and 514 nm were observed for 6a. Similarly emission band at 490 nm was observed for 6b, along the major emission band at 515 nm. The multi emission of organic fluorophores is in particular interesting for applications such as white light electroluminescence or luminescent bio imaging [7, 16–21]. The photophysical properties of the compounds are summarized in Table 1 and Figs. 1–9. Interestingly, 6a and 6b shows unexpected high fluorescence quantum yields (Φ=2.02 %) than 7a and 7b of the fluorophores that show excited state intramolecular proton transfer (ESIPT), which usually give quantum yield of less than 1 % [3, 4].

The solvent polarity dependence of the compounds' emission is studied (Figs. 1–9). For 6a and 6b the emission is greatly red-shifted in highly polar solvents such as methanol, DMF and DMSO. For 6a and 6b, the emission intensity is decreased by increasing the solvent polarity. We noticed that the dual emission of 6a and 6b are persistent in most solvents. Interestingly, we found that the intensity varied with the solvent polarity, but the emission wavelength did not change significantly. This property is different from the normal behavior of organic fluorophores that gives red-shifted emission in polar solvents [5, 18, 19]. We tentatively assign the increased emission intensity of 6a and 6b in polar solvents to a non-radiative decay channel which is enhanced by high polarity. Considering the potential ESIPT, the dual emission can be tentatively assigned to the enol, keto and hydro-phenazine form produced by the ESIPT (Fig. 10).

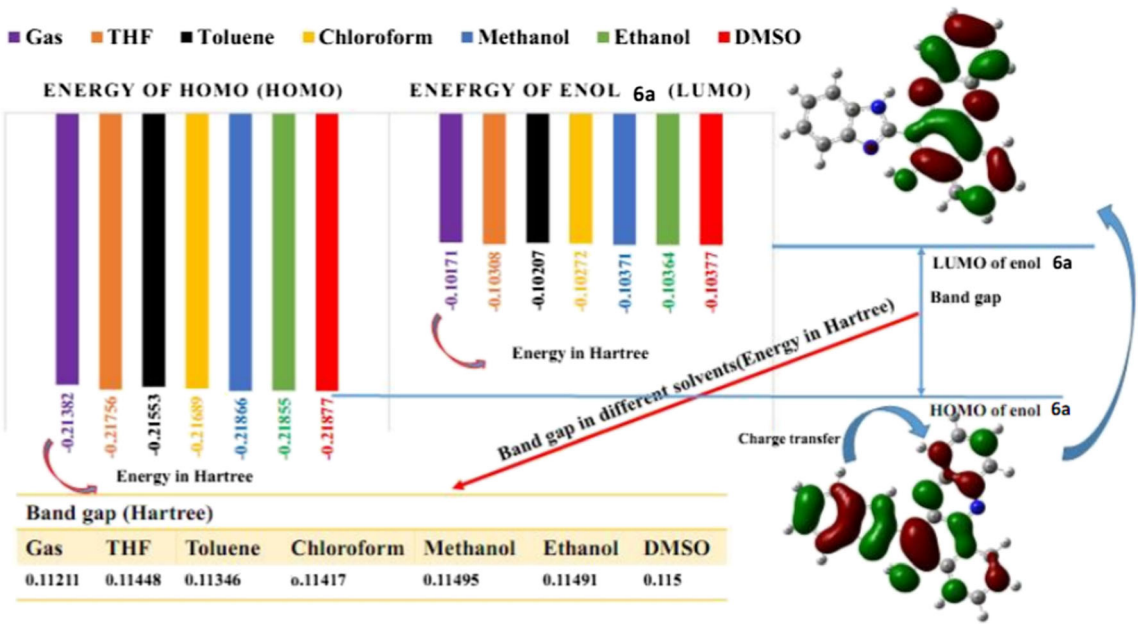

Gas	THF	Toluene	Chloroform	Methanol	Ethanol	DMSO
0.11211	0.11448	0.11346	o.11417	0.11495	0.11491	0.115

Fig. 13 Computed energy of HOMO and LUMO of enol 6a

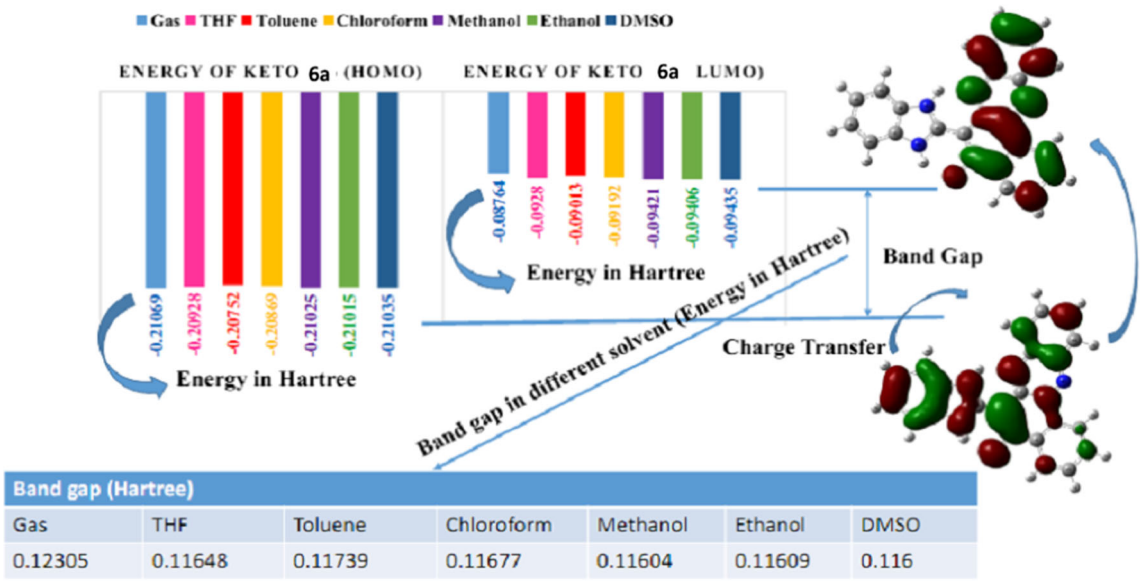

Band gap (Hartree)						
Gas	THF	Toluene	Chloroform	Methanol	Ethanol	DMSO
0.12305	0.11648	0.11739	0.11677	0.11604	0.11609	0.116

Fig. 14 Computed energy of HOMO and LUMO of Keto 6a

The ground state the dye 6a and 6b exists exclusively in its normal form as shown in Fig. 10 where the imine hydrogen of imidazole core is intra-molecularly hydrogen bonded to the imine nitrogen of phenazine core and hydroxy proton intra-molecularly bonded with the imine nitrogen of the imidazole core. On photo-excitation, the initially produced excited normal form (N*) undergoes a fast ESIPT process whereby one of the hydroxyl proton (at 1 or 8 position) is transferred from the hydroxyl group to the imine nitrogen along the pre-existing hydrogen bond, producing the excited tautomeric form of the dye. Accordingly, in the emission spectra, the short wavelength emission band is ascribed to the emission from the N* form and the long wavelength emission is ascribed to the emission from of excited tautomeric form of the dye. Such dual emissions are absent in the dyes 7a and 7b having chloro group Figs. 8 and 9.

Geomentry Optimization

Bond Length, Bond Angle and Energy of 6a and 6b

The computed bond lengths of the optimized enol and keto forms of 6a and 6b are given in Tables 1 and 2.

The structural changes due to ESIPT phenomenon in terms of bond angle, bond distance and geometry of the electron donor and acceptor groups are investigated by using optimized geometries as shown in Tables 2 and 3. The results of bond angle and bond length clearly indicate that, due to the intra-molecular hydrogen bonding the compounds has a six-member ring conformation in excited state (Fig. 10). The main feature of the molecular structures like stiochiometry, framework group, degree of freedom and point group of compounds remain the same in both enol and keto forms which can be deduced from Tables 2 to 3 for the compounds 6a and 6b. In Table 2 we list bond lengths (d) characterizing the N⋯H⋯O system in the enol and keto forms of 6a. The most important observation is that the distance between the N3 and O1 atoms is considerably longer in Enol 6a (in S0= 2.72 Å) than the Keto 6a (S0=2.60446 Å), vice versa in S1 state interatomic distance between N3 and O1 atom is shorter (S1=2.59 Å) in enol form than the Keto 6a (S1=2.60373 Å) by 0.01 Å. This is partly due to the increased rigidity of the Enol 6a in S1 state. Furthermore, the hydrogen bonding lengths in the Keto 6a (N3•••H9 i.e., S0=1.008, S1=0.995) and in Enol 6a (O1•••H9 i.e., S0=1.019, S1=1.020) longer in S0 and shorter in S1. The shorter distances have to be connected with stronger interactions in S1 Enol 6a than in S1 Keto 6a, and it seems to be the most probable reason for barriers for the proton transfer between the enol and keto forms of the molecule 6a. The computed dihedral and bond angle also reveals that S1 enol form having more planer arrangement than the keto form of 6a. The computed ground state energy of enol and keto form of 6a reveals that Keto 6a is more stable than Enol 6a in all solvents as shown in the Fig. S1. and energy difrence between the enol and keto form of 6a in eV and hartree depicted in Table 4 (Supporting information Fig. S1).

The change in bond length, dihedral angle, bond angle and ground state energy clearly indicates that ESIPT phenomenon is observed in compound 6a. For better understanding the ESIPT phenonmenone we optimized the three possible phototautomer of compound 6b i.e., (Keto 6b, Hyp 6b and

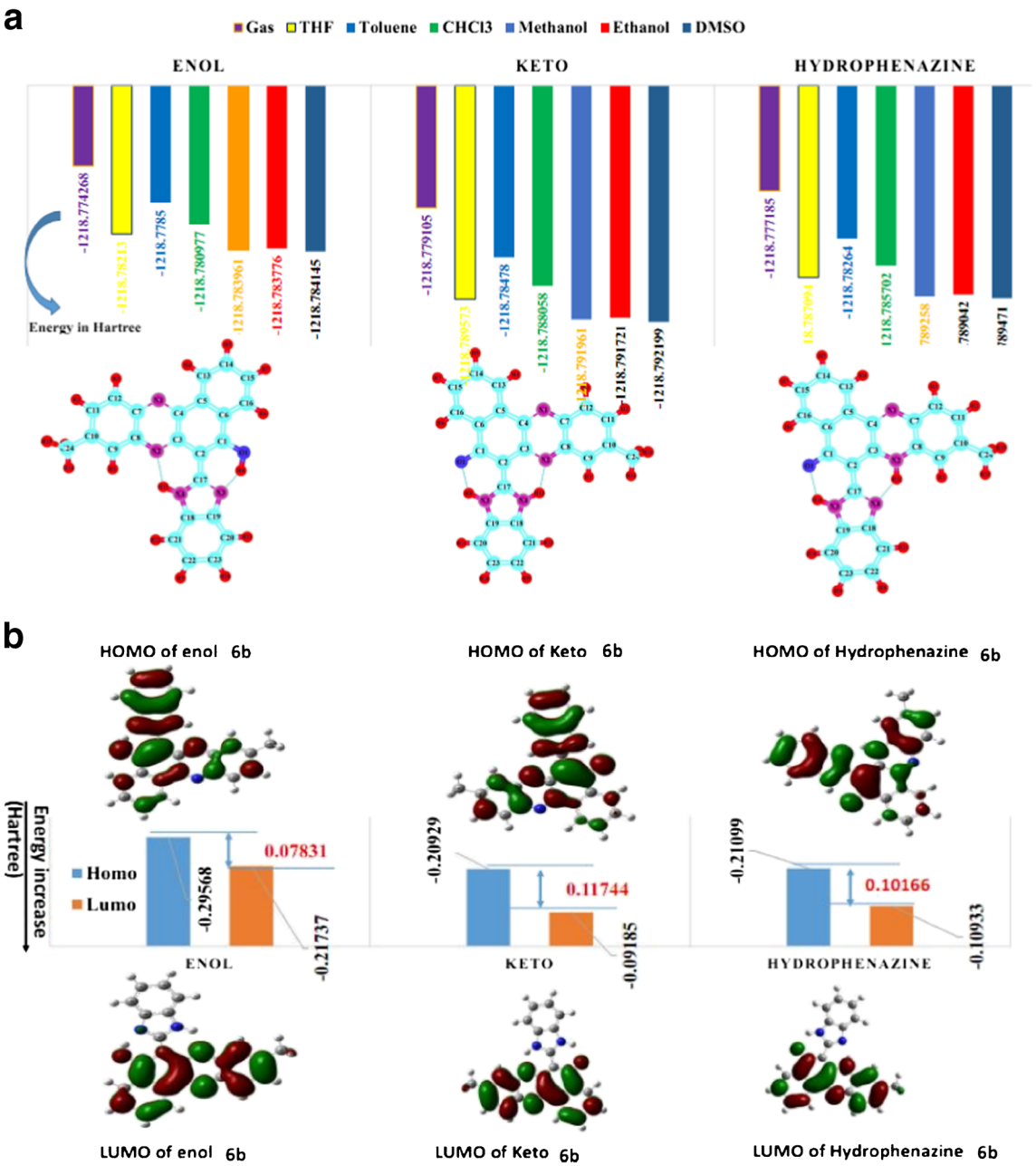

Fig. 15 Computed energy of HOMO and LUMO of enol 6b, keto 6b and Hyp 6b in difrent polarity of solvents

Enol 6b) as shown in the Fig. S2 and computed bond length, bond angle and ground state energy of enol 6b, Keto 6b and Hyp 6b are depicted Table 5.

From the Fig. S2 we observed that similar trends are observed for compounds 6b. The compounds 6a and 6b are roughly planar in enol and keto forms and this facilitates the ESIPT. The 5,6 benzene-fused benzophenazine core increases the acidity of hydroxyl group present in the ring. This is further confirmed by our computational study. In enol form, the lone pair of electrons present on oxygen is involved in resonance, the single bond length character is converted in to double bond character hence the bond length between O-H decreases as compared to the keto form. This is also observed for the other compounds. The changes in bond length, bond angle and dihedral angle due to excited state intramolecular phenomenon for all the compounds are summarized in Tables 3 and 4. The optimized three possible tautomers of the compound 6b are shown in the Fig. 11 and their computed energy values are shown in the Table 5 in different polarity of solvents. As the polarity of the solvents increses the ground

Table 6 Energy of HOMO and LUMO of enol 6b, keto 6b and Hyp 6b in difrent polarity of solvents

Solvent	Enol 6b			Keto 6b			Hydrophenazine 6b		
	HOMO enol	LUMO enol	difference	HOMO Keto	LUMO Keto	difference	HOMO Hyp	LUMO Hyp	difference
DMSO	−0.29568	−0.21737	0.07831	−0.20929	−0.09185	0.11744	−0.21099	−0.10933	0.10166
Methanol	−0.21798	−0.10119	0.11679	−0.20918	−0.09171	0.11747	−0.21087	−0.10926	0.10161
Ethanol	−0.21786	−0.10112	0.11674	−0.20907	−0.09156	0.11751	−0.21076	−0.1092	0.10156
THF	−0.21681	−0.10048	0.11633	−0.20809	−0.09022	0.11787	−0.20975	−0.1086	0.10115
Chloroform	−0.21606	−0.10005	0.11601	−0.20742	−0.08929	0.11813	−0.20904	−0.1082	0.10084
Toluene	−0.2145	−0.09922	0.11528	−0.20605	−0.08734	0.11871	−0.20756	−0.1074	0.10016
Gas	−0.21225	−0.09839	0.11386	−0.20428	−0.0845	0.11978	−0.20546	−0.10658	0.09888

state energy of the Enol 6b, Keto 6b and Hyp 6b decreses. It means that polar solvent stabilizes the ground state of above mentioned tautomer of 6b. Similar trend was observed for the compound 6a as shown in the Table 2. Form the Table 4 it is seen that the keto tautomer has less energy than the enol and hydrophenazine forms of 6b. Hence the compounds 6a and 6b are more stable in thw keto form than than the enol and the hydrophenazine forms of 6b (Fig 12).

Frontier Molecular Orbitals

The different frontier molecular orbitals were studied to understand the electronic transition and charge delocalization within these ESIPT chromophores. The comparative increase and decrease in the energy of the occupied (HOMO's) and virtual orbitals (LUMO's) gives a qualitative idea of the excitation properties and the ability of hole or electron injection. First allowed and the strongest electron transitions with largest oscillator strength usually correspond almost exclusively to the transfer of an electron from HOMO→LUMO. The energy of HOMO, LUMO and band gap of the enol 6a and Keto 6b shown in Figs. 13 and 14 from which it is observed that the bang gap of the keto 6a is more as compared to the enol 6a. Similar trend was found for the keto 6b, Hyp 6b and enol 6b as shown in the Figs. 15a and b, Table 6.

We observed that the ground state of the keto from of 6a has lower energy than the keto form of 6a. And for the compound 6b : the order of energy of tautomers is keto> hydrophenazine>enol, the keto form has less energy as compared to the hydrophenazine form. In both the compounds 6a and 6b the keto tautomer is found to be more stable as compared to the hydrophenazine and the enol form. The bond

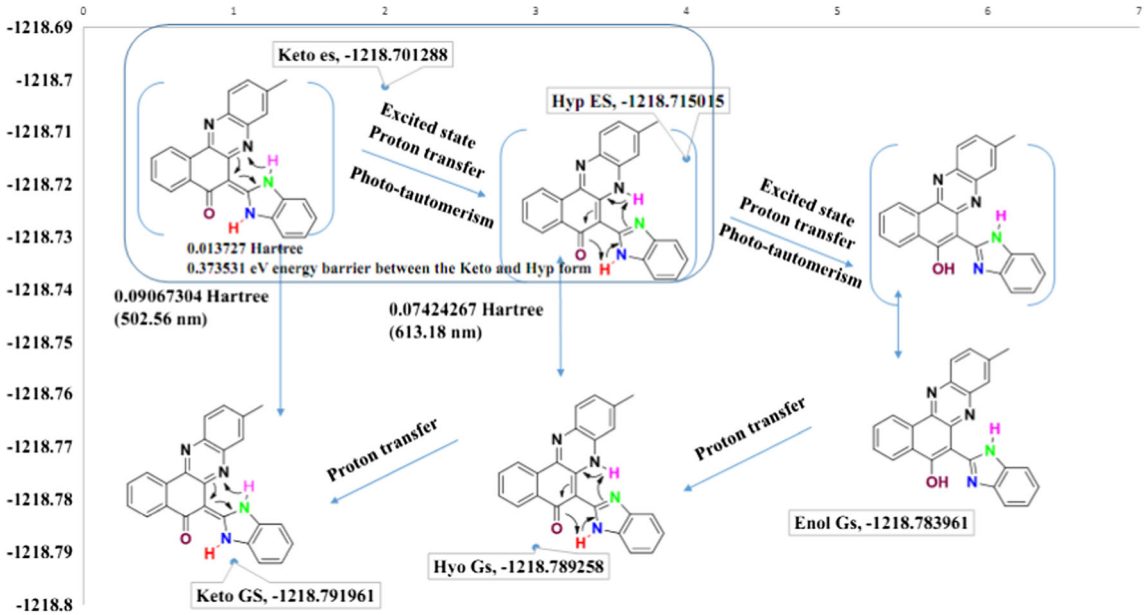

Fig. 16 Possible ESIPT phenonmenone in dye 6b

length and bond angle computation clearly indicate that the proton transfer is possible (Fig. 10).

The energy barrier between the keto and hydrophenazine form of 6b is quite less as shown in the Fig. 16. Hence the keto and hydrophenazine tautomer may give emission due to the barrierless ESIPT and the second emission is due to the proton transfer in the excited state form of Hyp 6b to Enol 6b as shown in Fig. 16.

Conclusion

Photo-physical properties of 6-(1H-benzo[d]imidazol-2-yl)benzo[a]phenazin-5-ol derivatives were studied in solvents of different polarities. The absorption and emission wavelengths were computed using TD DFT and they are in good agreement with the experimental results, the HOMO-LUMO gap for each compound is the same in all the solvents. The compounds 6a and 6b show dual emission, an intense peak at short wavelength and a shoulder peak at long wavelength in DMSO, methanol, acetone and acetonitrile. In case of chloroform a shoulder peak at short wavelength and an intense peak at long wavelength was observed. The compounds 7a and 7b did not show dual emission in all the solvents. The compounds show a large Stokes shift due to ESIPT process and this can be important in designing fluorescence probes. The computational methods have been useful for assignments of the absorption and emission and thus lead to more understanding at molecular level and this is not possible by experiments alone.

Acknowledgments The author Amol S. Chaudhari is thankful to university grand commission (UGC-CAS), New Delhi, India for providing financial support. Sharad R. Patil is grateful to CSIR-UGC, New Delhi, India for providing financial support.

References

1. Corbellini VA, Scroferneker ML, Carissimi M, Rodembusch FS, Stefani VA (2010) fast and cost-effective methodology for Fonsecaea pedrosoi ATCC46428 staining using ESIPT fluorescent dyes. J Photochem Photobiol B 99:126–132
2. Zamotaiev OM, Postupalenko VY, Shvadchak VV, Pivovarenko VG, Klymchenko AS, Mély Y (2011) Improved hydration-sensitive dual-fluorescence labels for monitoring peptide-nucleic acid interactions. Bioconjug Chem 22:101–107
3. Vazquez RS, Rodrıguez MC, Mosquera M, Rodrıguez-Prieto F (2008) Rotamerism, tautomerism, and excited-state intramolecular proton transfer in 2- (4 ′ - N, N -diethylamino-2 ′ -hydroxyphenyl) benzimidazoles : novel benzimidazoles undergoing excited-state intramolecular coupled proton and charge transfer. J Phys Chem A 112: 376–387
4. Neuwahl FVR, Bussotti L, Buntinx G, Ascq Ï (2008) Ultrafast proton transfer in the S state of 1277–83
5. Sun W, Li S, Hu R, Qian Y, Wang S, Yang G (2009) Understanding solvent effects on luminescent properties of a triple fluorescent ESIPT compound and application for white light emission. J Phys Chem A 113:5888–5895
6. Chipem FAS, Krishnamoorthy G (2009) Comparative theoretical study of rotamerism and excited state intramolecular proton transfer of 2- (2 ′ -Hydroxyphenyl) benzimidazole, and 8- (2 ′ -Hydroxyphenyl) purine photophysics and rotamerization were examined theoretically by a comparative stu. 12063–70
7. Links DA. (2012) Excited state intramolecular proton transfer (ESIPT): from principal photophysics to the development of new chromophores and applications in fluorescent molecular probes and luminescent materials. 8803–17
8. Sakai K-I, Takahashi S, Kobayashi A, Akutagawa T, Nakamura T, Dosen M et al (2010) Excited state intramolecular proton transfer (ESIPT) in six-coordinated zinc (ii)-quinoxaline complexes with ligand hydrogen bonds: their fluorescent properties sensitive to axial positions. Dalton Trans 39:1989–1995
9. Paterson MJ, Robb MA, Blancafort L, DeBellis AD (2005) Mechanism of an exceptional class of photostabilizers: a seam of conical intersection parallel to excited state intramolecular proton transfer (ESIPT) in o-hydroxyphenyl-(1,3,5)-triazine. J Phys Chem A 109:7527–37
10. Ghiggino KP, Scully AD, Leaver IH (1986) Effect of solvent on excited-state intramolecular proton transfer in benzotriazole photostabilizers. J Phys Chem 90:5089–93
11. Luxami V, Kumar S (2008) Molecular half-subtractor based on 3,3′-bis(1H-benzimidazolyl-2-yl) [1,1′] binaphthalenyl-2,2′-diol. New J Chem 32:2074
12. Cardoso MB, Samios D, da Silveira NP, Rodembusch FS, Stefani V, Rodembusch S (2007) ESIPT-exhibiting protein probes: a sensitive method for rice proteins detection during starch extraction. Photochem Photobiol Sci 6:99–102
13. Vaswani KG, Ker MD, Road MP (2009) Detection of aqueous mercuric ion with a structurally simple 8-hydroxyquinoline derived ON-OFF fluorosensor. Inorg Chem 48:5797–5800
14. Poteau X, Saroja G, Spies C, Brown RG (2004) The photophysics of some 3-hydroxyflavone derivatives in the presence of protons, alkali metal and alkaline earth cations. J Photochem Photobiol A Chem 162:431–439
15. Renschler CL, Harrah LA (1985) Nucl Inst Methods Phys Res A A235:41
16. Yang G, Li S, Wang S, Li Y (2011) Emissive properties and aggregation-induced emission enhancement of excited-state intramolecular proton-transfer compounds. Compt Rendus Chim 14:789–798
17. Yao D, Zhao S, Guo J, Zhang Z, Zhang H, Liu Y et al (2011) Hydroxyphenyl-benzothiazole based full color organic emitting materials generated by facile molecular modification. J Mater Chem 21: 3568
18. Kwon JE, Park SY (2011) Advanced organic optoelectronic materials : harnessing excited-state intramolecular proton transfer (ESIPT) process. Adv Mater 23:3615–3642
19. Wu J, Liu W, Ge J, Zhang H, Wang P (2011) Chem Soc Rev New sensing mechanisms for design of fluorescent chemosensors emerging in recent years. Chem Soc Rev 3483–95
20. Buyukcakir O, Bozdemir OA, Kolemen S, Erbas S, Akkaya EU (2009) Tetrastyryl-Bodipy dyes: convenient synthesis and characterization of elusive near IR fluorophores. Org Lett 11:4644–4647
21. Zhang X, Yu H, Xiao Y (2012) Replacing phenyl ring with thiophene: an approach to longer wavelength Aza-dipyrromethene boron difluoride (Aza-BODIPY) dyes. J Org Chem 77:669–673
22. Tian Z, Tian B, Zhang J (2013) Synthesis and characterization of new rhodamine dyes with large Stokes shift. Dye Pigment 99:1132–1136

23. Rurack K, Spieles M (2011) Fluorescence quantum yields of a series of red and near-infrared dyes emitting at 600–1000 nm. Anal Chem 83:1232–1242
24. Patil VS, Padalkar VS, Tathe AB, Gupta VD, Sekar N (2013) Synthesis, photo-physical and DFT studies of ESIPT inspired novel 2-(2′,4′-dihydroxyphenyl) benzimidazole, benzoxazole and benzothiazole. J Fluoresc 23:1019–29
25. Frisch MJ, Trucks GW, Schlegel HB, Scuseria GE, Robb MA, Cheeseman JR et al (2010) Gaussian 09, revision C.01. Gaussian, Inc, Wallingford CT
26. Treutler O, Ahlrichs R (1995) Efficient molecular numerical integration schemes. J Chem Phys 102:346–354
27. Becke AD (1993) A new mixing of Hartreee Fock and local density-functional theories. J Chem Phys 98:1372–1377
28. Lee C, Yang W, Parr RG (1988) Development of the Colle-Salvetti correlation-en- ergy formula into a functional of the electron density. Phys Rev B 37:785–789
29. Hehre WJ, Radom L, Schleyer PR, Pople JA (1986) Ab initio molecular orbital theory. Wiley, New York
30. Bauernschmitt R, Ahlrichs R (1996) Treatment of electronic excitations within the adiabatic approximation of time dependent density functional theory. Chem Phys Lett 256:454–64
31. Furche F, Rappaport D (2005) Density functional theory for excited states: equilibrium structure and electronic spectra. In: Olivucci M (ed) Computational photochemistry. Elsevier, Amsterdam, p 16, Chapter 3
32. Tomasi J, Mennucci B, Cammi R (2005) Quantum mechanical continuum salvation models. Chem Rev 105:2999–3094